



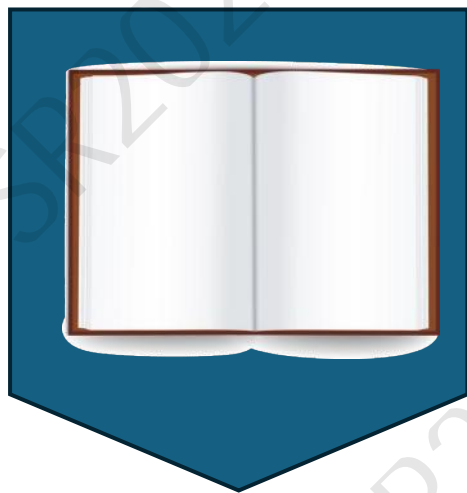
# **Thermal stress analysis of ladle refractory under coupled temperature and stress fields based on ANSYS software**

Reporter: Xie Chongchong

Advisor: Tian Lin



# CONTENT



1

Introduction

2

Research idea and calculation method

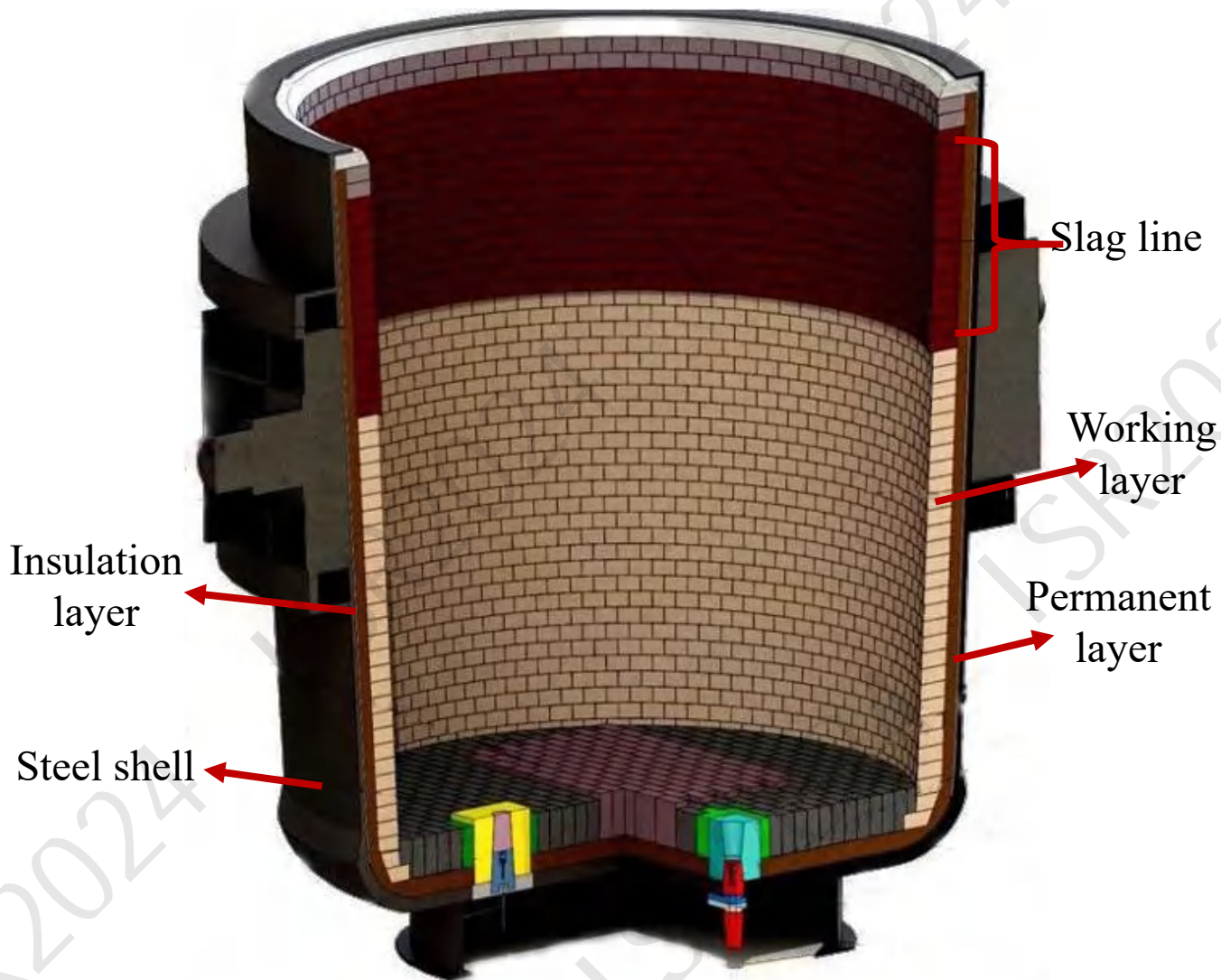
3

Simulation analysis

4

Conclusion

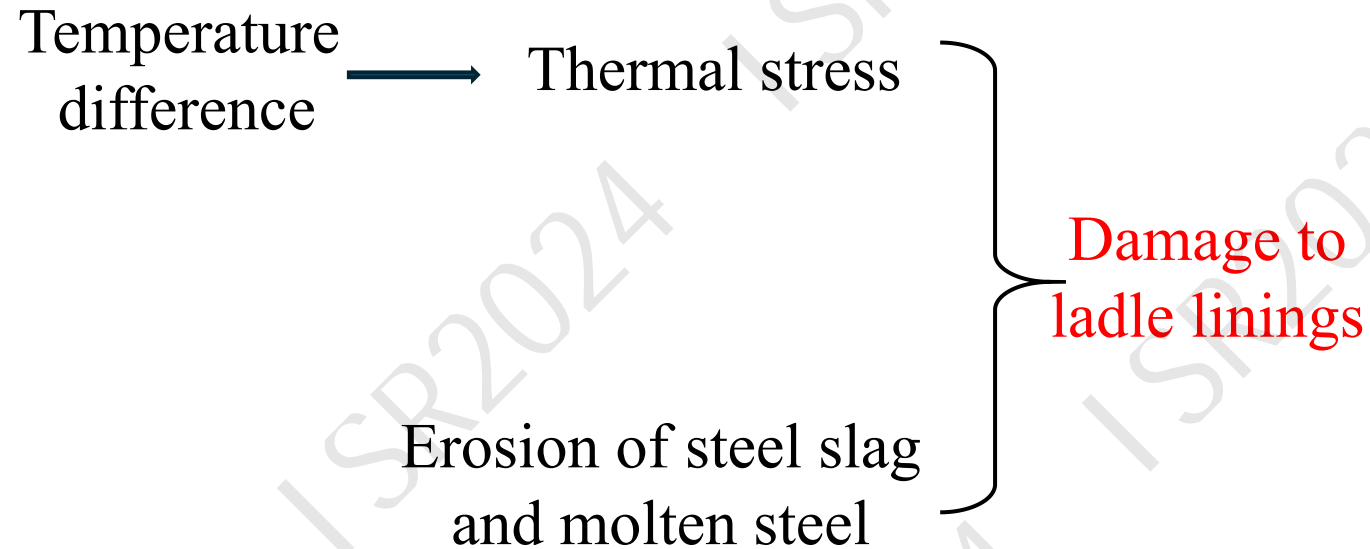
## 1.1 Introduction of ladle



Steel ladle is an important equipment in steelmaking, which has the multi-functional roles of liquid steel heat preservation, container transportation, temporary smelting and so on .

Fig.1 Diagram of the ladle structure

## 1.2 Purpose and significance of the study



In the actual production process, there is no relevant equipment to measure the thermal stress of the ladle.

In order to predict and lengthen the ladle life, I use the ANSYS software to simulate and calculate the temperature distribution and thermal stress distribution in the ladle lining.

I am able to find the location of the maximum thermal stress in the ladle by simulating, Then we adjust the refractory configuration.

## 2.1 Research idea

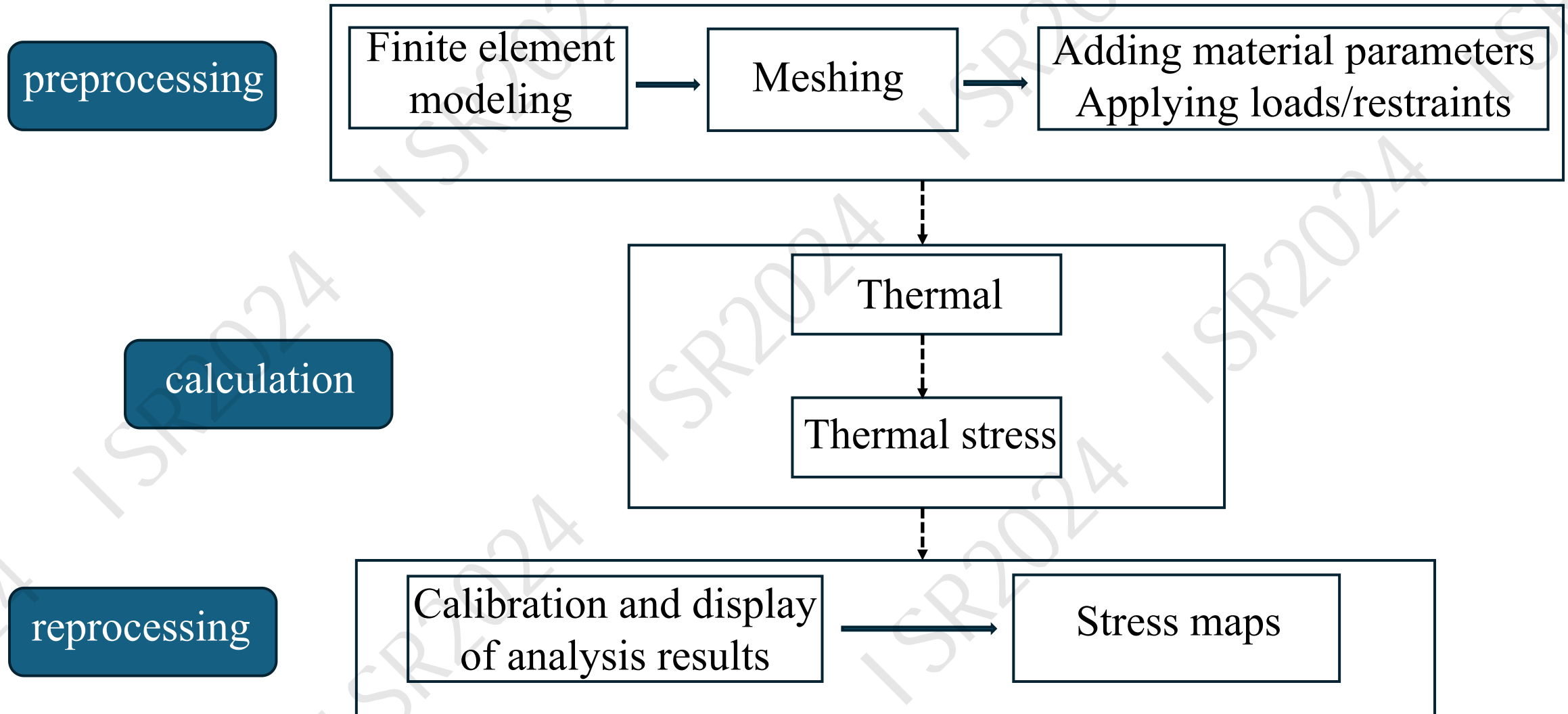


Fig.2 Flowchart of research idea

## 2.1 Research idea

### (1) Finite element modeling

- ① Due to the small inclination of the actual ladle wall to the bottom of the ladle, the model of the ladle is simplified to a cylinder.
- ② Neglecting the effects of permeable turns at the bottom of the ladle, sliding spouts and drives.

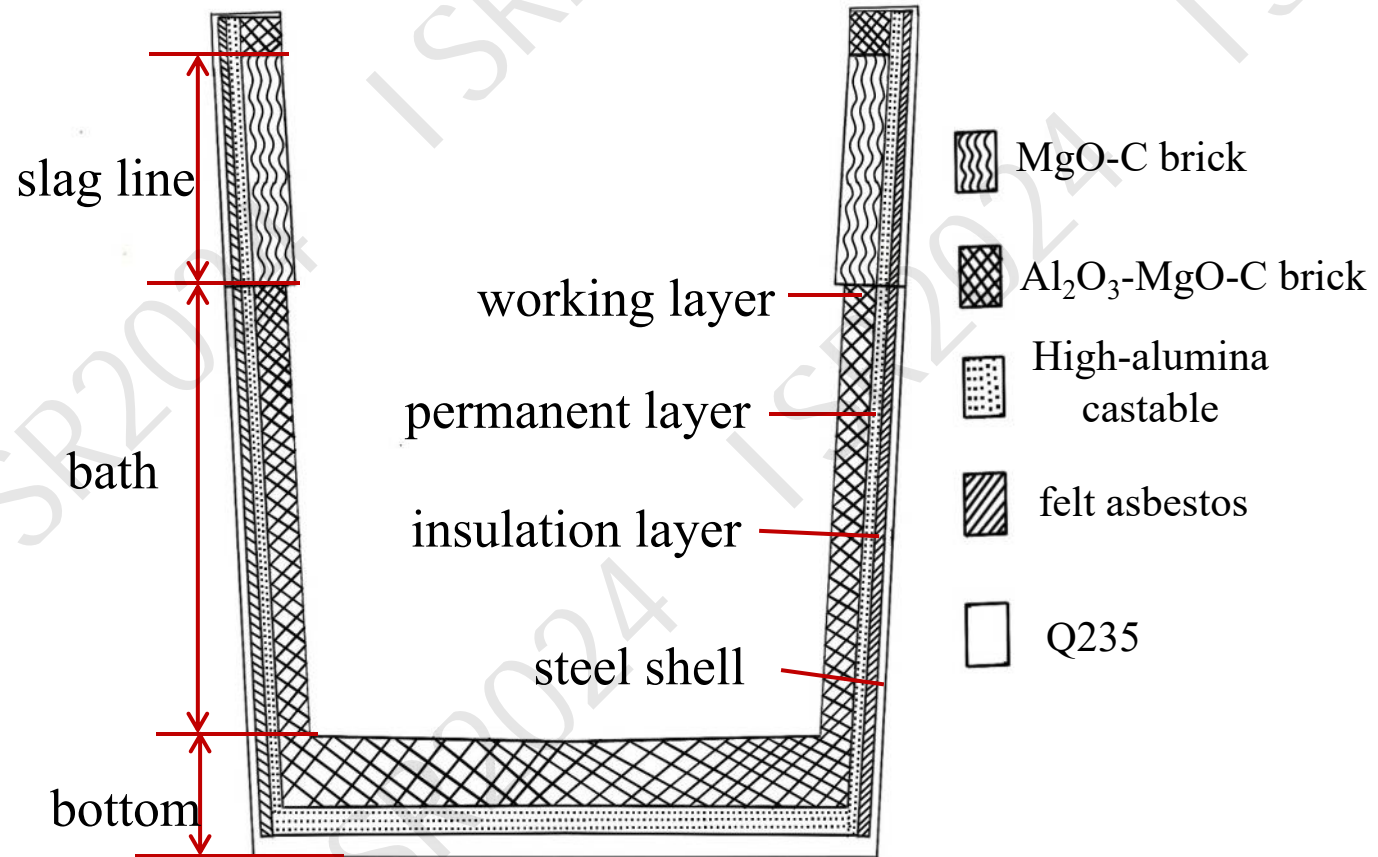


Fig.3 Diagram of structure of ladle lining materials

## 2.1 Research idea

### (2) Meshing

- ① Using hexahedral meshing
- ② Setting the 100mm cell size



### (3) Material parameters adding

Table 1 Physical parameters of refractory materials for ladle linings

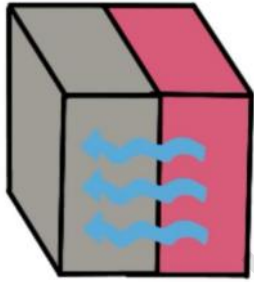
|  | temperature<br>°C        | MgO-C brick  | Al <sub>2</sub> O <sub>3</sub> -MgO-C<br>brick | High-alumina<br>castable | felt<br>asbestos | steel<br>shell |
|--|--------------------------|--------------|--|--------------------------|------------------|----------------|
| density/kg·m <sup>-3</sup>                                     | ordinary<br>temperatures | 3100         | 2950   | 2800                     | 1150             | 7850           |
| thermal<br>conductivity<br>W·(m·K) <sup>-1</sup>               | <1000<br>≥1000           | 13.6<br>12.0 | 3<br>3   | 0.713<br>0.713           | 0.126<br>0.126   | 34<br>31       |
| specific heat<br>J·(Kg·K) <sup>-1</sup>                        | <1000<br>≥1000           | 960<br>960   | 800<br>1200                                    | 900<br>1500              | 815<br>815       | 460<br>460     |
| thermal<br>coefficient of<br>expansion<br>(×10 <sup>-6</sup> ) | ordinary<br>temperatures | 10.2         | 5  | 5.8                      | 1.2              | 13.7           |
| elasticity<br>modulus /MPa                                     | ordinary<br>temperatures | 10200        | 6300   | 5700                     | 2000             | 20600<br>0     |
| Poisson's ratio  | ordinary<br>temperatures | 0.21         | 0.21   | 0.21                     | 0.01             | 0.3            |

Fig.4 Meshing diagram of the ladle

## 2.2

# Calculation Method

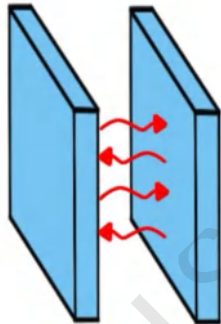
Heat transfer method



heat conduction

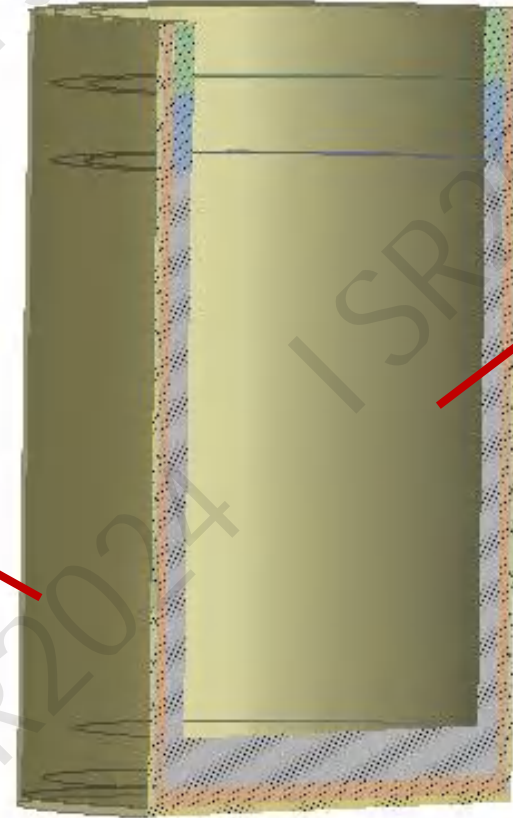


heat convection



heat radiation

### Boundary conditions



Boundary conditions of category I

Boundary conditions of category III

## 3.1 Temperature field analysis

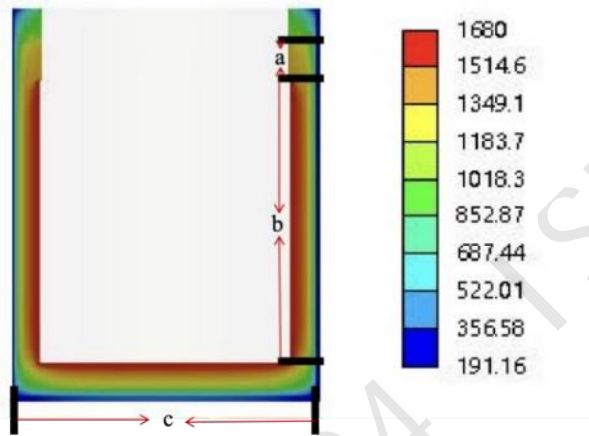


Fig.5 Cloud diagram of the temperature distribution of the ladle overall



Fig.6 Cloud diagram of the temperature distribution in the slag line

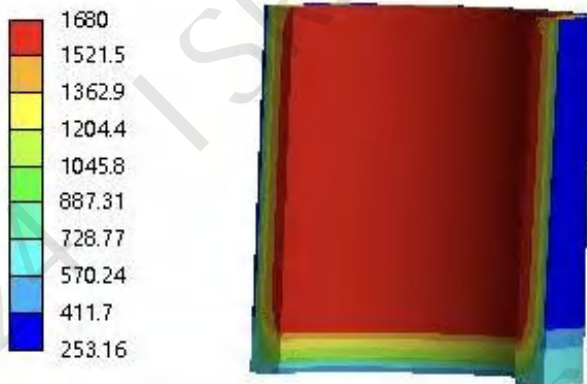


Fig.7 Cloud diagram of the temperature distribution in the bath

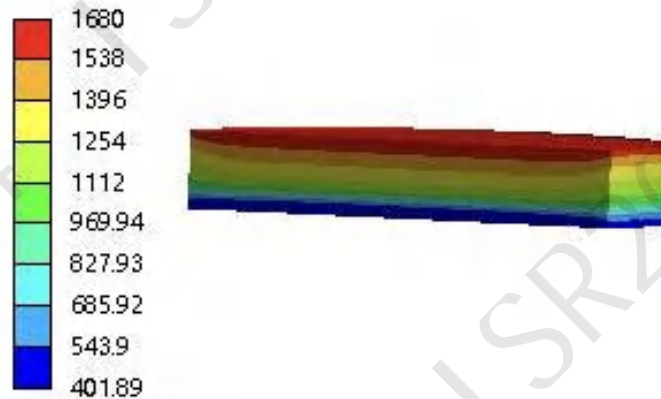


Fig.8 Cloud diagram of the temperature distribution at the bottom the ladle

the temperature at the bottom of the steel shell is higher than that at the wall of the steel shell.

## 3.1 Temperature field analysis

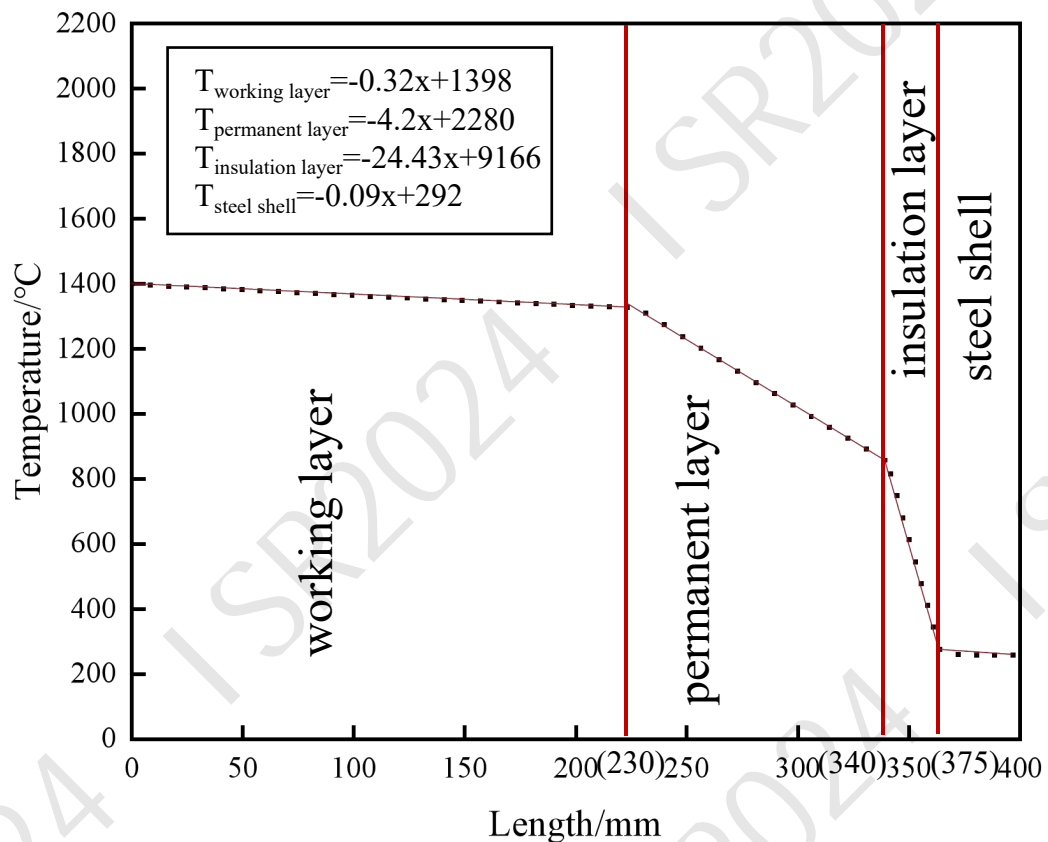


Fig.9 Temperature variation diagram of slag line

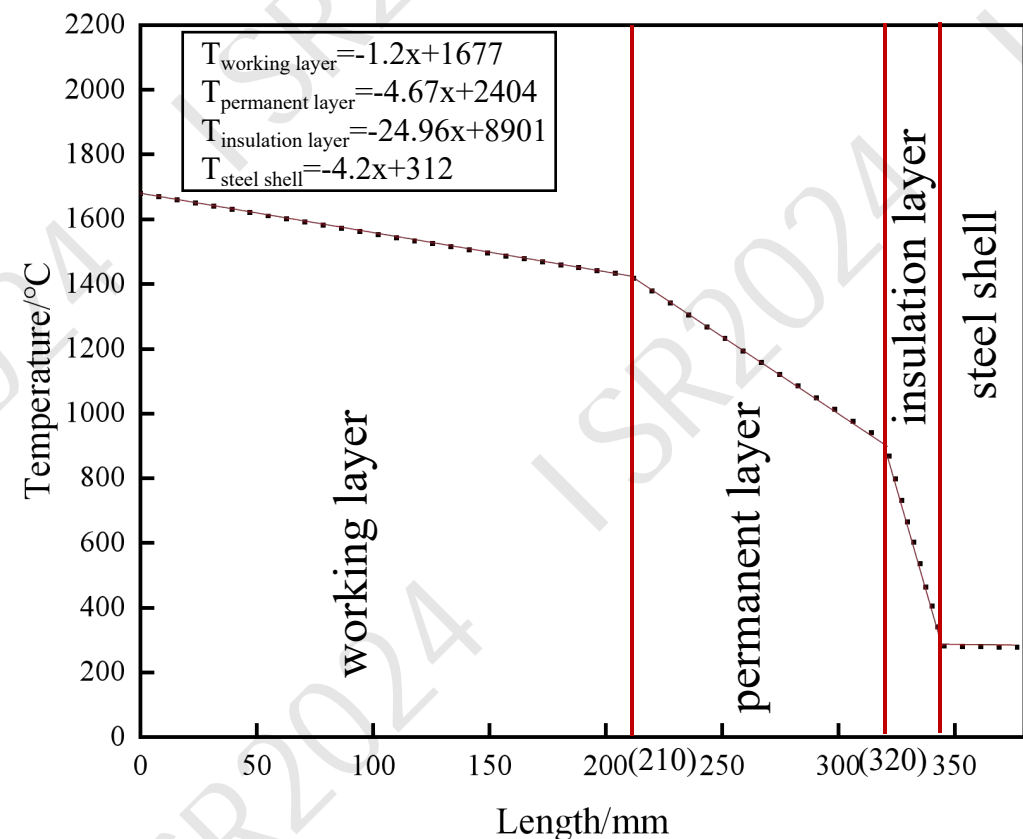
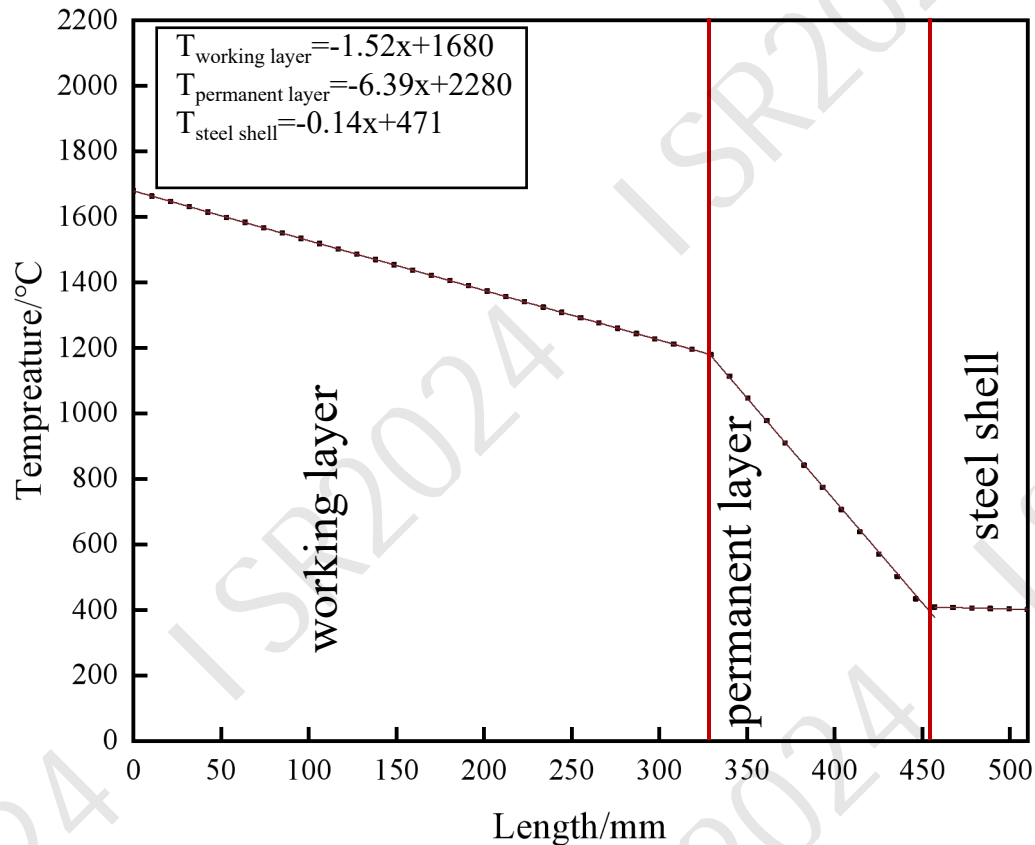


Fig.10 Temperature variation diagram of the bath

## 3.1 Temperature field analysis



Temperature at different locations in the linings of the three regions varied linearly with distance from the working face.

Fig.11 Temperature variation diagram at the bottom of the ladle

## 3.2 Thermal Stress Analysis

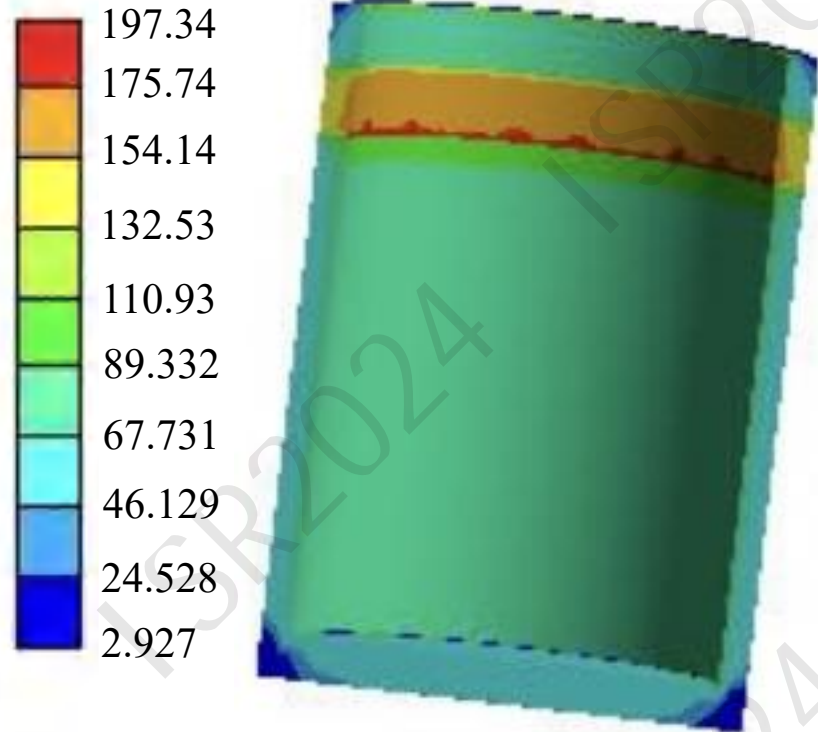


Fig.12 Cloud map of thermal stress distribution in the working layer

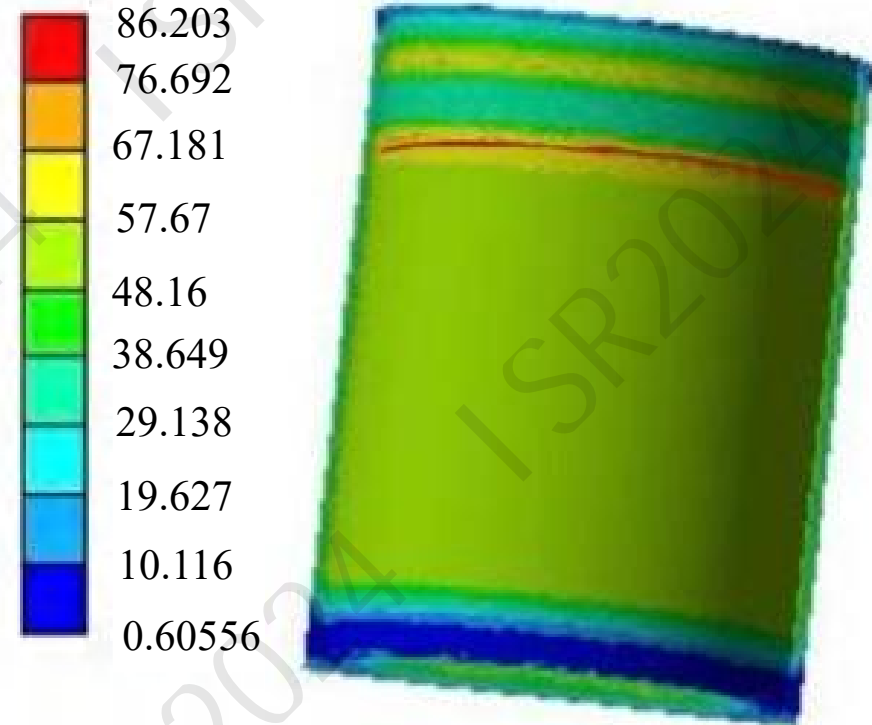
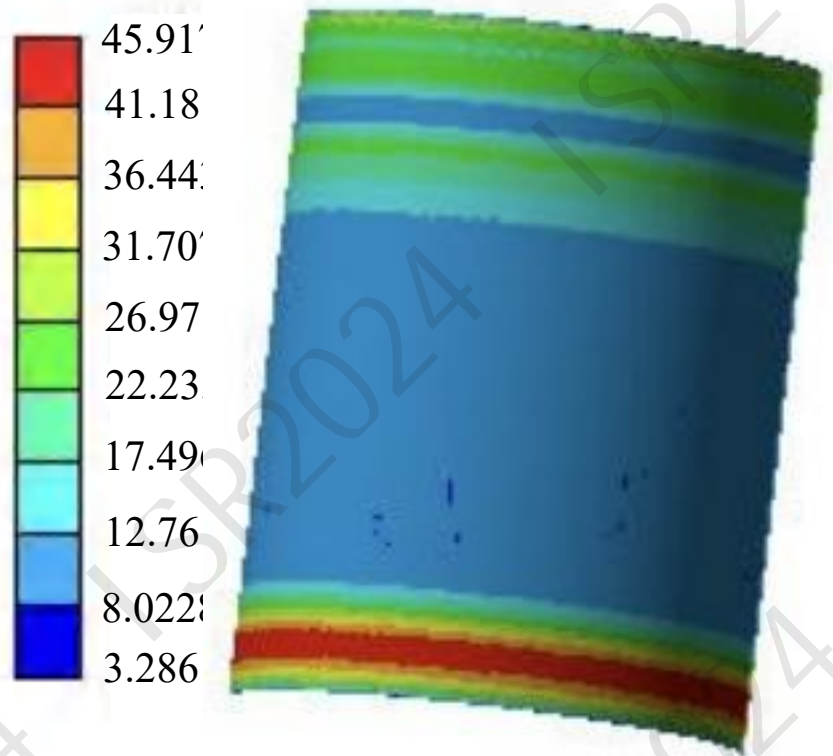


Fig.13 Cloud map of thermal stress distribution in the permanent layer

## 3.2 Thermal Stress Analysis



Maximum thermal stress in the working layer is at the slag line ;  
The maximum thermal stress in the permanent layer is behind working layer of slag line;  
The maximum thermal stress of the insulation layer is at bottom of the insulation layer.

Fig.14 Cloud map of thermal stress distribution in the insulation layer

### 3.3 Microstructure analysis

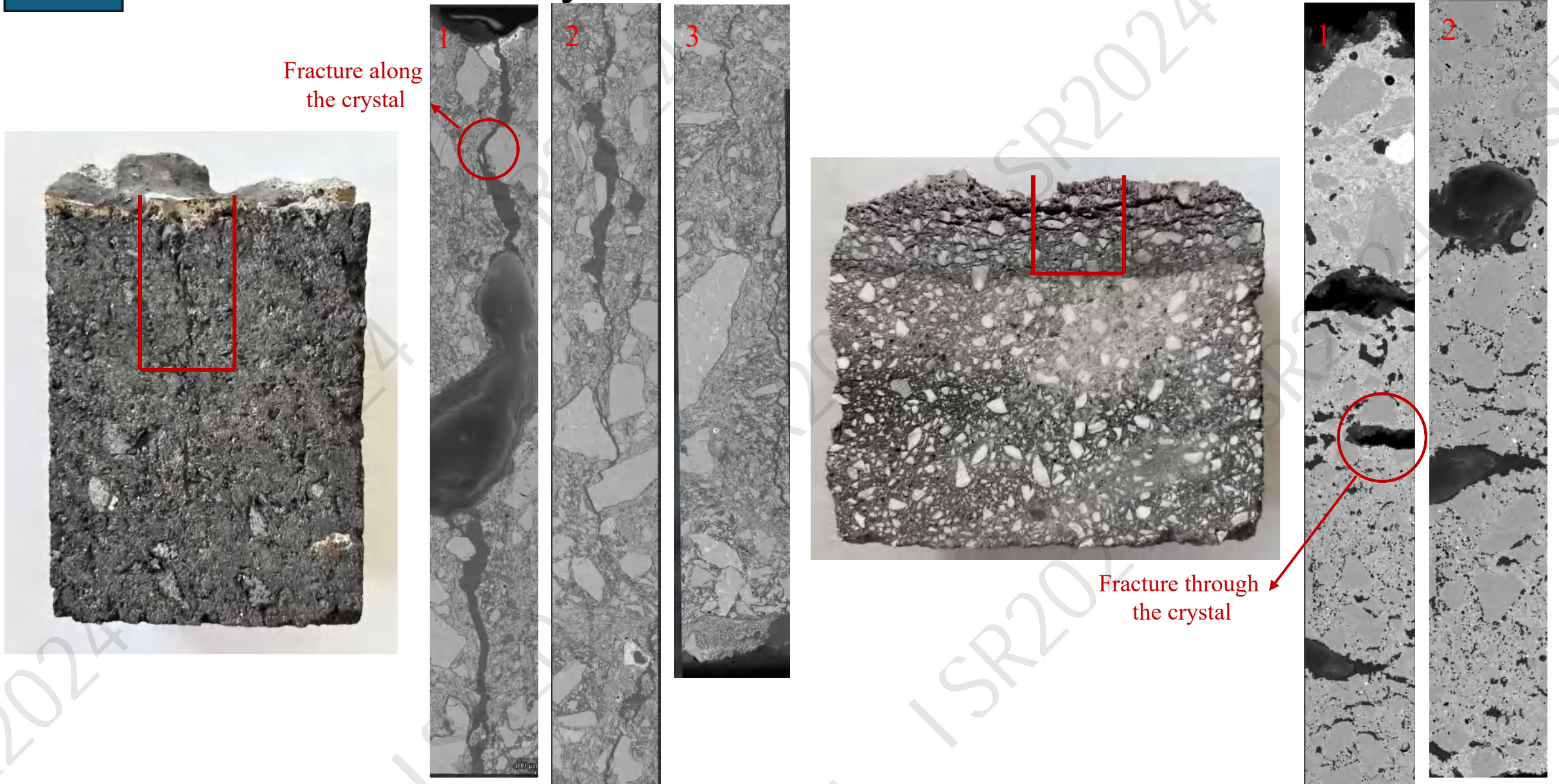
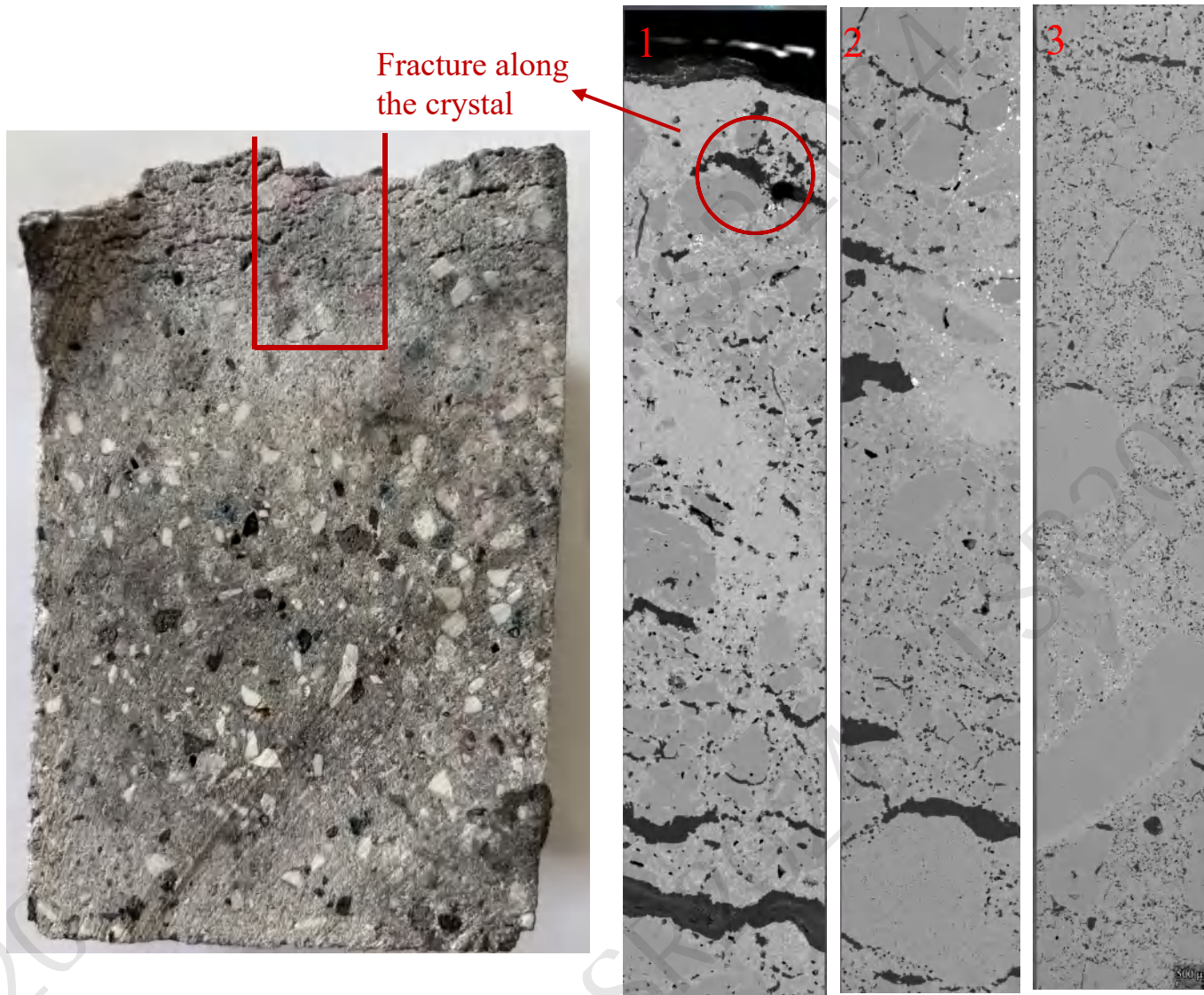


Fig.15 Macrostructure and microstructure graphs of bricks used in the slag line and the bath

### 3.3 Microstructure analysis



There are cracks in the bricks used because of the thermal stress. And then according to the continuous microstructure diagrams, these can be seen that cracks are generated from the working surface to the non-working surface. In addition, they get smaller and smaller until disappear. Cracks suffer chemical attack first of matrix and then of filling agent.

**These conclusions are consistent with the simulation results.**

Fig.16 Macrostructure and microstructure graphs of bricks used at the bottom of the ladle

## 4 Conclusion

---

(1) The temperature in different regions is slightly different, the temperature at the bottom of the ladle is higher than that at the wall of the ladle. And the temperature of the ladle lining in the same material is linearly distributed. The temperature of each part of the ladle can be predicted according to the fitted linear equation.

(2) The maximum thermal stress of the ladle appears at the slag line and decreases with distance from the working face. And the slag line is subjected to the highest thermal stress, resulting in cracking the largest crack.

(3) In addition, the microstructure graphs are consistent with the simulation results. Furthermore, we can optimize the areas of most damaged based on the simulation results, strengthening its resistance to compression and erosion.



遼寧科技大學

University of Science and Technology Liaoning

thank you for listening!

Reporter: Xie Chongchong

Advisor: Tian Lin